Textile-reinforced mortar (TRM) versus fibre-reinforced polymers (FRP) in flexural strengthening of RC beams

Saad M. Raoof [a,b,*], Lampros N. Koutas [c], Dionysios A. Bournas [d]

[a] Department of Civil Engineering, University of Nottingham, NG7 2RD Nottingham, UK
[b] Department of Civil Engineering, University of Tikrit, Tikrit, Iraq
[c] Department of Civil and Structural Engineering, University of Sheffield, S1 3JD Sheffield, UK
[d] European Commission, Joint Research Centre (JRC), Directorate for Space, Security and Migration, Safety and Security of Buildings Unit, via E. Fermi 2749, I-21027 Ispra, Italy

HIGHLIGHTS

- TRM was compared to FRP in flexural strengthening of RC beams.
- TRM was almost as effective as FRP when debonding governed the failure.
- Effectiveness of TRM versus FRP was improved by increasing the number of layers.
- Epoxy coated textiles resulted in increased efficiency of TRM system.
- TRM debonding stress was predicted using a formula developed for FRP systems.

ARTICLE INFO

ABSTRACT

This paper compares the flexural performance of reinforced concrete (RC) beams strengthened with textile-reinforced mortar (TRM) and fibre-reinforced polymers (FRP). The investigated parameters included the strengthening material, namely TRM or FRP; the number of TRM/FRP layers; the textile surface condition (coated and uncoated); the textile fibre material (carbon, coated basalt or glass fibres); and the end-anchorage system of the external reinforcement. Thirteen RC beams were fabricated, strengthened and tested in four-point bending. One beam served as control specimen, seven beams strengthened with TRM, and five with FRP. It was mainly found that: (a) TRM was generally inferior to FRP in enhancing the flexural capacity of RC beams, with the effectiveness ratio between the two systems varying from 0.46 to 0.80, depending on the parameters examined, (b) by tripling the number of TRM layers (from one to three), the TRM versus FRP effectiveness ratio was almost doubled, (c) providing coating to the dry textile enhanced the TRM effectiveness and altered the failure mode; (d) different textile materials, having approximately same axial stiffness, resulted in different flexural capacity increases; and (e) providing end-anchorage had a limited effect on the performance of TRM-retrofitted beams. Finally, a simple formula proposed by *fib* Model Code 2010 for FRP reinforcement was used to predict the mean debonding stress developed in the TRM reinforcement. It was found that this formula is in a good agreement with the average stress calculated based on the experimental results when failure was similar to FRP-strengthened beams.

1. Introduction and background

Over the last decades, the issue of upgrading and structural strengthening the existing reinforced concrete (RC) infrastructure has become of great importance. This is due to deterioration of these structures as a result of ageing, environmental conditions, lack of maintenance, and the need to meet the current design codes requirements (i.e. Eurocodes). Over the last two decades, the use fibre-reinforced polymers (FRP) for retrofitting concrete structures, has gain popularity among other conventional strengthening systems (such as steel/RC jacketing). However, some drawbacks have been observed with the use of FRPs, which are mainly associated to the use of epoxy resins. These drawbacks include high cost, inability to apply on wet surfaces or at low ambient temperature, low

* Corresponding author at: Department of Civil Engineering, University of Nottingham, NG7 2RD Nottingham, UK.
E-mail addresses: Saad.Raoof@nottingham.ac.uk (S.M. Raoof), L.Koutas@sheffield.ac.uk (L.N. Koutas), Dionysios.BOURNAS@ec.europa.eu (D.A. Bournas).

permeability to water vapour, and poor behaviour at high temperatures.

To overcome these drawbacks, a new alternative cement-based composite material, known as textile-reinforced mortar (TRM), has been suggested for external strengthening of structures [1,2]. A TRM is a composite comprises high-strength fibres made of carbon, basalt or glass in form of textiles embedded into inorganic materials such as cement-based mortars. The textiles typically consist of fibre rovings woven or stitched at least in two orthogonal directions, thus creating an open-mesh geometry. TRM composite is also identified with other acronyms such as TRC [3], and FRCM [4]. Several advantages of TRM are associated with the use of cement-based mortars including: resistance to high temperatures [5,6], low cost, ability to be applied in an environment of low temperatures or on a wet surface, permeability to water vapour, and compatibility with concrete substrates.

In the last few years, a significant number of studies have been directed towards investigating possible exploitation of TRM in several cases of retrofitting RC structural elements. Bond between TRM and concrete substrate has been investigated in many studies [7–14]. TRM jacketing has also been applied as a mean of external strengthening of RC structures in the following cases: confinement of RC columns (i.e. [1]), shear retrofitting of RC elements [2,15–19], confinement of RC columns subjected to seismic load (e.g. [20–24]), reinforcing of infilled RC frames subjected to seismic load [25], flexural strengthening of one-way (e.g. [26–28]) and two-way [29] RC slabs. The results indicated that TRM is a promising alternative to FRP in retrofitting structures. Examples of real applications of TRM worldwide in the construction field can be found in [30].

Research on the flexural performance of RC beams strengthened with TRM has been reported in [31–37]. Parameters investigated in these studies, were; the textile-fibre materials, for example, carbon-fibre textiles in [31,33,37], polyparaphenylene benzobisoxazole (PBO)-fibre textiles in [32–34,37], and basalt-fibre textile [35]; the number of layers [32–37]; the strengthening configuration [33]; the compressive strength of concrete [36]; and the type of textile-fibre materials [37]. The main conclusions of these studies were: (a) application of TRM to RC beams considerably improved their flexural capacity [31–37]; (b) increasing the number of TRM layers had twofold effect: increased the flexural capacity and altered the failure mode [32,37].

The comparison between TRM and FRP strengthening system in enhancing the flexural capacity of RC beams has been only reported in a few number of studies. In the study of Triantafillou and Papanicolaou, 2005 [31] it was found, on the basis of only two specimens, that TRM was 30% less effective than FRP, with the observed failure mode being different (rupture of fibres for the FRP-strengthened beam and interlaminar debonding for the TRM-strengthened beam). Elsanadedy et al., 2013 [35] reported that, the performance of TRM strengthening system in enhancing the flexural capacity of RC beams was slightly less than that for FRP system. But TRM system is more efficient in increasing the

deformation capacity. This conclusion was made based on the comparison between two tested beams only; one beam strengthened with five layers of TRM in form of U-shaped jacket made of basalt-fibre textile and another retrofitted with one layer of basalt FRP.

Based on the above, it is clear that more research is needed to cover the subject of the effectiveness of TRM versus FRP in flexural strengthening of RC beams. The aim of this paper is to compare the effectiveness of the two strengthening systems in enhancing the flexural capacity of RC beams. Parameters considered were: the number of strengthening layers (1, 3, 5, and 7), the textile surface condition (coated or uncoated), the textile-fibre material (carbon, coated basalt or glass fibres), and the strengthening configuration (end-anchorage).

2. Experimental programme

2.1. Test specimens and investigated parameters

The objective of the present study was to evaluate the performance of TRM versus FRP in increasing the flexural capacity of RC beams. For this purpose, thirteen half-scale beams of rectangular section with dimensions of 101 mm width and 202 mm depth were fabricated, strengthened and tested under 4-point flexure. The length of the beams was 1675 mm (Fig. 1a), whereas the clear flexural and shear span were 1500 mm and 580 mm, respectively (Fig. 1b).

All beams were intentionally designed with a low amount of longitudinal reinforcement ratio (ρ_s = 0.56%) in order to simulate flexural-deficient beams. The internal steel reinforcement comprised two 8 mm-diameter deformed bars in tension and two 12 mm deformed bars positioned in compression (Fig. 1). The transversal reinforcement comprised 8 mm-diameter steel stirrups at a distance of 80 mm along the two shear spans of the beams, (expect for the constant moment zone), resulting - by design – to a shear resistance seven times higher than the shear force corresponding to the predicted flexural capacity of the unstrengthened beam. In all beams, the concrete cover was same and equal to 15 mm.

The investigated parameters were: (a) the reinforcement material (TRM vs FRP), (b) the number of TRM/FRP layers (one, three, five, and seven), (c) the material of the textile-fibres (carbon, glass and basalt), (d) the coating of the textile (coated carbon-fibre versus dry carbon-fibre textile), and (e) the end-anchorage of the externally bonded composite layers (U-jacketing). Table 1, with the support of Fig. 2, provide a description of the tested specimens. The notation of the strengthened specimens is BN_F, where B represents the type of binder (R for epoxy resin, and M for cement mortar), N refers to the number of TRM or FRP layers and F denotes the type of textile fibres (C for dry carbon fibres, CCo for coated carbon fibres, BCo for coated basalt fibres and G for glass fibres). For the specimens retrofitted with U-jackets at their ends, an additional suffix (EA, standing for end-anchorage) is added to the notation. The description of the specimens follows:

- CON: unstrengthened beam which served as control specimen.
- R1_C and M1_C: beams strengthened with 1 dry carbon FRP and TRM layer, respectively.
- M1_ CCo: beam strengthened with 1 coated carbon TRM layer.
- R3_C and M3_C: beams strengthened with 3 dry carbon FRP and TRM layers, respectively.
- M5_C: beam strengthened with 5 dry carbon TRM layers.
- R7_BCo and M7_BCo: beams strengthened with 7 coated basalt FRP and TRM layers, respectively.
- R7_G and M7_G: beams strengthened with 7 dry glass FRP and TRM layers, respectively.
- R3_C_EA and M3_C_EA: 3 dry carbon FRP and TRM layers strengthened beam, anchored at their ends with two dry carbon FRP and TRM layers, respectively.
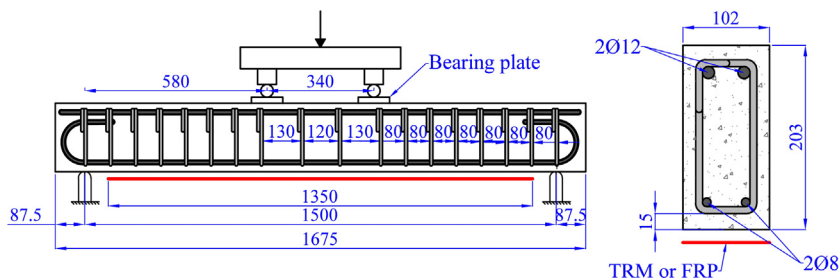
Fig. 1. Details of test beams (dimensions in mm).

Table 1
Strengthening configuration and materials properties of test specimens.

Specimen	t^* (mm)	No. of layers	Measured thickness of TRM (mm)	Ratio of axial stiffness**	ρ_f^{***} (%)	Concrete Strength (MPa)	
						Compressive strength$^+$	Tensile splitting strength$^+$
CON	–	–		–	–	19.9 (0.5)	2.1 (0.06) +
TRM-retrofitted							
M1_C	0.095	1	3	1	0.0475	19.9 (0.5)	2.1 (0.06)
M1_CCo	0.095	1	5	1	0.0475	19.9 (0.5)	2.1 (0.06)
M3_C	0.095	3	6	3	0.1425	19.9 (0.5)	2.1 (0.06)
M5_C	0.095	5	10	5	0.2375	19.9 (0.5)	2.1 (0.06)
M7_BCo	0.0371	7	17	1.06	0.1299	19.9 (0.5)	2.1 (0.06)
M7_G	0.044	7	12	1.07	0.1540	19.9 (0.5)	2.1 (0.06)
M3_C_EA	0.095	3	7	3	0.1425	21.7 (0.3)	2.4 (0.05)
FRP-retrofitted							
R1_C	0.095	1		1	0.0475	21.7 (0.3)	2.4 (0.05)
R3_C	0.095	3		3	0.1425	21.7 (0.3)	2.4 (0.05)
R7_BCo	0.0371	7		1.06	0.1299	21.7 (0.3)	2.4 (0.05)
R7_G	0.044	7		1.07	0.1540	21.7 (0.3)	2.4 (0.05)
R3_C_EA	0.095	3		3	0.1425	21.7 (0.3)	2.4 (0.05)

* Textile nominal thickness.
** Axial stiffness of bare coated basalt or glass fibres textiles (axial stiffness of one layer times the number of layers) divided by the axial stiffness of one layer of dry carbon fibres textile.
*** Textile reinforcement ratio (as a percentage) which calculated as follows: $\rho_f = A_f /bh$, where b and h are the width and depth of the beam respectively. A_f is the cross sectional area of the textile fibres, the area of fibres is the product of $t'b$, where t is the equivalent thickness of textile fibres and b is the beam width.
$^+$ Standard deviation in parenthesis.
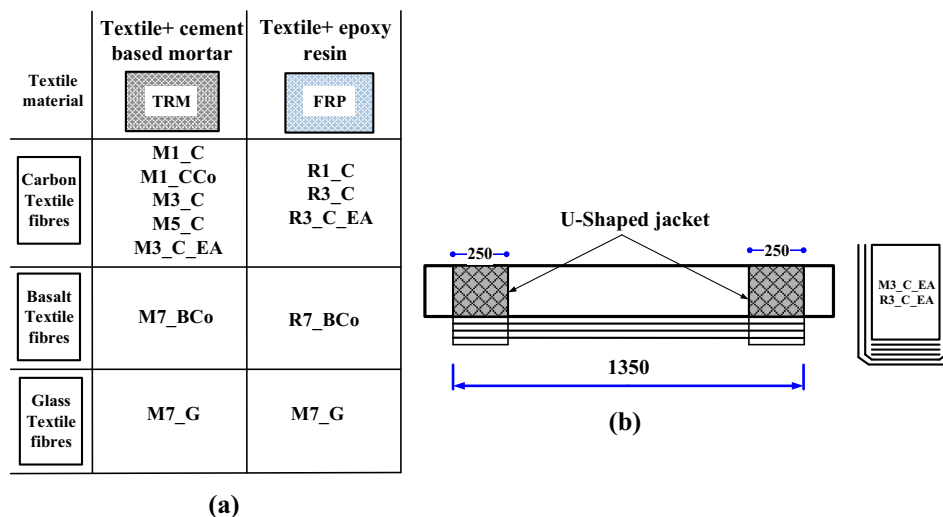
Fig. 2. (a) Group of specimens; (b) details of end anchorage system (dimensions in mm).

2.2. Materials properties

The beams were cast on two different dates using the same mix design of concrete. The compressive and splitting tensile strength of the concrete were determined on the day of testing. Three concrete cylinders (dimensions of 150 mm-diameter and 300 mm-height) were tested according to the EN 12390-3 and EN 12390-6 standards [38,39], respectively. The results are presented in Table 1.

The yield stress, ultimate strength, and ultimate strain of the 8 mm-diameter steel bars (which used for the tension and shear links reinforcement) was 569 MPa, 631 MPa and 7.85%, respectively. The yield stress, ultimate strength, and ultimate strain of the 12 mm-diameter bars (compression reinforcement) were 561 MPa, 637 MPa and 12.8%, respectively. These values were obtained experimentally by testing three identical specimens of each type of bars.

Three different textiles (Fig. 3) were used as external reinforcement, namely carbon-fibre textile (dry and coated), glass-fibre textile (dry) and basalt fibre-textile (coated). All textiles made of fibre rovings distributed equally in two orthogonal directions. Details of the textiles, such as weight, mesh size and equivalent thickness (calculated based on the equivalent smeared distribution of fibres), are presented in Fig. 3. It is noted that seven layers of glass-fibre or coated basalt-fibre textile have approximately the same axial stiffness with one dry carbon textile layer.

The binder of the TRM composite was cement-based with added polymers at a ratio of 8:1 by weight. The water to binder ratio was 0.23, resulting in a good workability and plastic consistency. The compressive and flexural strength of the mortar were obtained on the day of testing according to EN 1015-11 [40] on three mortar prisms with 40 × 40 mm cross section and 160 mm length. The average flexural and compressive strengthen of the mortar were 39.2 MPa, and 9.8 MPa, respectively. For those specimens strengthened with FRP, an epoxy resin consisted of two parts with a mixing ratio of 4:1 by weight was used as binder. According to the product data-sheet, the tensile strength and modulus of elasticity of this adhesive was 30 MPa and 3.8 GPa, respectively.

For the specimen strengthened with coated carbon fibre textile (M1_CCo), prior to strengthening the textile was impregnated with a low viscosity, two-part epoxy resin. The tensile strength and the elastic modulus of this adhesive were 72.4 MPa and 3.18 GPa, respectively (according to the material data sheets). The procedure of coating the dry carbon textile included, impregnating the textile with this epoxy using a plastic roll. The coated textiles were left to cure for two days before using them for strengthening.

Uniaxial tensile tests were conducted on TRM and FRP coupons comprising one textile layer, in order to evaluate the main mechanical properties of the composite materials. Three identical specimens (coupons) were tested for each type of textile material. The geometry and test setup of both FRP and TRM coupons is shown in
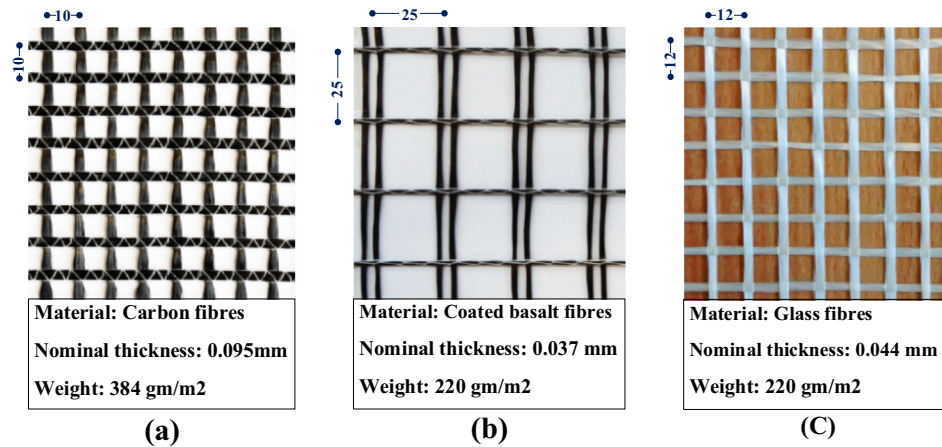
Fig. 3. Textiles used in this study: (a) carbon fibres textile; (b) glass fibres textile; (c) coated basalt fibres textile (dimensions in mm).

Fig. 4a and b, respectively. The FRP coupons had a rectangular shape and were designed according to the requirements of ACI 440.3R-33 code [41]. The TRM coupons had a dumbbell geometry and the test setup used was a modification of the setups adopted in [3,42]. The gauge length of the FRP and TRM coupons was 300 mm and 240 mm respectively. A monotonic load was applied under displacement control at a rate of 2 mm/min.

All coupons failed due to fibres rupture at the central region of the gauge length. Fig. 4c shows typical stress-strain curves of both FRP and TRM coupons made of one layer of dry carbon fibres textile. As shown in this figure, the stress- strain curve of FRP coupon comprises linear behaviour up to failure, whereas the corresponding curve of TRM coupon is characterised by two distinct stages: (1) linear elastic behaviour until the first crack occurs in the mortar, and (2) non-linear stage (cracking stage) with progressively decreasing slope (due to mortar cracking) up to failure due to fibres rupture.

Table 2 reports the mean values of ultimate tensile stress (f_{fu}), ultimate strain (ε_{fu}), and modulus of elasticity (E_f). The ultimate tensile stress (f_{fu}) (presented in Table 2) was calculated by dividing the ultimate load to the cross-sectional area of the FRP or TRM coupon in the direction of loading. The cross-sectional area of

the coupon was calculated by multiplying the width of the coupon (same width of the textile) by the nominal thickness of the fibre presented in Table 1. The value of elastic modulus of FRP was calculated directly from the stress- strain curves by dividing the ultimate tensile stress (f_{fu}) to the corresponding ultimate strain (ε_{fu}) because the behaviour was linear up to failure. The corresponding value of TRM was calculated as the secant modulus of elasticity of the stress-strain curve during the 2nd stage of response (modulus of elasticity of the cracked section), which is the slope of the line connecting the point corresponding to the initiation of cracking stage and the point corresponding to the maximum tensile stress.

It is worth mentioning that, the strength values of FRP composite was higher than that of the corresponding TRM composite comprising the same textile materials (Table 2). This is mainly attributed to the degree of impregnation of the fibres with the binding material. In FRP composites, the degree of impregnation of fibres in a roving is extremely good, whereas in TRM composites it is only the outer filaments of a roving that are impregnated with the binding material. This results in fracture of a portion of the fibres, while the core ones experience a degree of slippage.
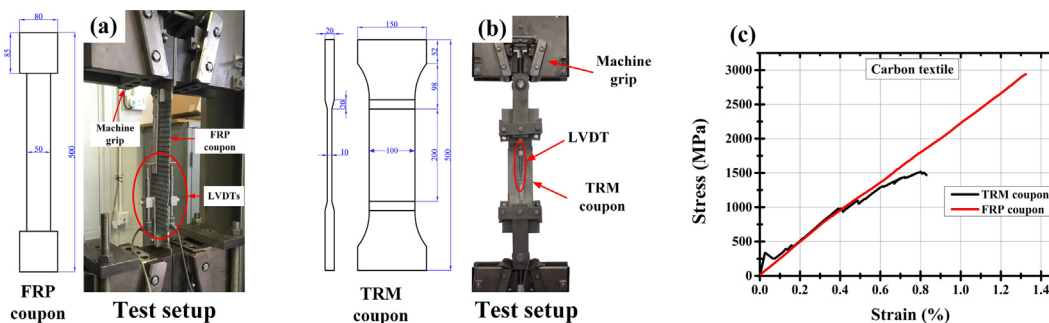
Fig. 4. (a) Geometry of FRP coupons and test setup (all dimensions in mm); (b) Geometry of TRM coupons and test setup (all dimensions in mm); (c) typical tensile stress-strain curves of the tested TRM and FRP.

Table 2
Mechanical properties of TRM and FRP coupons made of one layer of textile fibres.

Textile-fibres materials	TRM coupon				FRP coupon			
	No. of bundles	f_{fu}[a] (MPa)	ε_{fu}[b] (%)	E_f[c] (GPa)	No. of bundles	f_{fu}[a] (MPa)	ε_{fu}[b] (%)	E[c] (GPa)
Carbon	10	1518 (7.4)*	0.793 (0.03)*	166.8 (4.7)*	6	2936 (31.5)*	1.33 (0.03)*	219 (4)*
Coated carbon	10	2843 (25.3)*	1.39 (0.03)*	200.5 (3.9)*	6	n.a.	n.a.	n.a.
Coated basalt	5	1190 (20.0)*	1.825 (0.02)*	63.7 (1.7)*	3	1501 (15.0)*	1.508 (0.02)*	99.5 (2.6)*
Glass	8	794 (9.0)*	1.66 (0.03)*	41.1 (0.9)*	5	1019 (31)*	1.02 (0.05)*	93.3 (8)*

* Standard deviation in parenthesis.
[a] f_{fu}: ultimate tensile stress (MPa), calculated by dividing the maximum load recorded with the cross-sectional area of the textile fibres in the loading direction.
[b] ε_{fu}: ultimate tensile strain (%).
[c] E_f: modulus of elasticity (GPa).

2.3. Strengthening procedure

The strengthening material (TRM or FRP) was externally bonded to the bottom of the beams over a length of 1350 mm (see Fig. 1 and Fig. 2b). The strengthening procedure for both strengthening systems had the characteristics of a typical wet lay-up application and comprised the following steps:

- Prior to strengthening, the concrete surface was prepared as follows: for FRP strengthened beam, the surface was roughened using a grinding machine and the resulted concrete surface was cleaned from dust with compressed air (fig. 5a); For TRM-strengthened specimens, a 50-mm grid of grooves with a depth of approximately 3 mm was made using a grinding machine, in order to improve the bond with concrete substrate. Finally, the concrete surface was cleaned with compressed air (Fig. 5b).
- The procedure for application of TRM materials included: (a) dampening the concrete surface with water; (b) application of a layer of mortar with approximately 2-mm-thickness (Fig. 5c); (c) application of the textile into the mortar, and gently pressing with hand to ensure good impregnation with cement mortar (Fig. 5d).
- The procedure for FRP-retrofitted specimens included: application of the textile over a thin layer of resin and then impregnated with resin using a plastic roll (Fig. 5e).
- The above procedure for both strengthening systems was repeated in case of more than one textile layers were applied.
- For TRM-retrofitted beams, the final layer of textile was covered with a final layer of mortar with approximately 3 mm thickness and levelled (Fig. 5f).

Similar surface preparation was used for the specimens received U-shaped TRM or FRP end strips as an anchorage system (M3_C_EA, R3_C_EA), as shown in Figs. 5g and h. The application of the two layered U-jackets commenced immediately after the application of the longitudinal external reinforcement.

2.4. Experimental setup

All beams were subjected to four point bending as shown in Fig. 6a–b. The clear span was 1500 mm, and the selected configuration resulted in a 340 mm-long constant moment zone and a 580 mm-long shear span (Fig. 6a). The load was applied using a servo-hydraulic actuator (100 kN capacity) which was vertically fixed on a stiff reaction frame (Fig. 6b). The load was applied monotonically under displacement control at a rate of 1 mm/min. Two LVDTs were fixed at the mid-span of the beam (one on each side) to measure independently the mid-span deflection. Two bearing plates with square dimensions of 100 mm and 25 mm thickness were fixed under the points of load application to prevent the local failure of the beams due to concrete crushing.

3. Experimental results

The main results of all tested beams are presented in Table 3, including: (1) The cracking load (P_{cr}). (2) The yield load (P_y) (which is defined as the load corresponding to the steel yielding). (3) The ultimate recorded load (P_u). (4) The displacement corresponding to cracking load (δ_{cr}). (5) The displacement corresponding to the yielding load (δ_y) (average mid-span deflection from two LVDTs corresponding to Py). (6) The displacement at ultimate load (δ_u) (average of mid-span deflection from two LVDTs at the ultimate load (Pu). (7) The flexural capacity increase due to strengthening. (8) The observed failure mode.

3.1. Load–deflection curves

The load-deflection curves of all tested beams are presented in Fig. 7a–d. All curves in Fig. 7 were characterised by three distinct stages (ascending branches with decreasing slope) up to the maximum load: (1) Stage I: un-cracked beam; (2) Stage II: development of cracking up to yielding of the steel reinforcement; and (3) Stage III: post-yielding response up to failure.

Any difference between the curves of the retrofitted beams and the control one (Fig. 7), is attributed to the contribution of strengthening materials to the flexural performance of the beams.
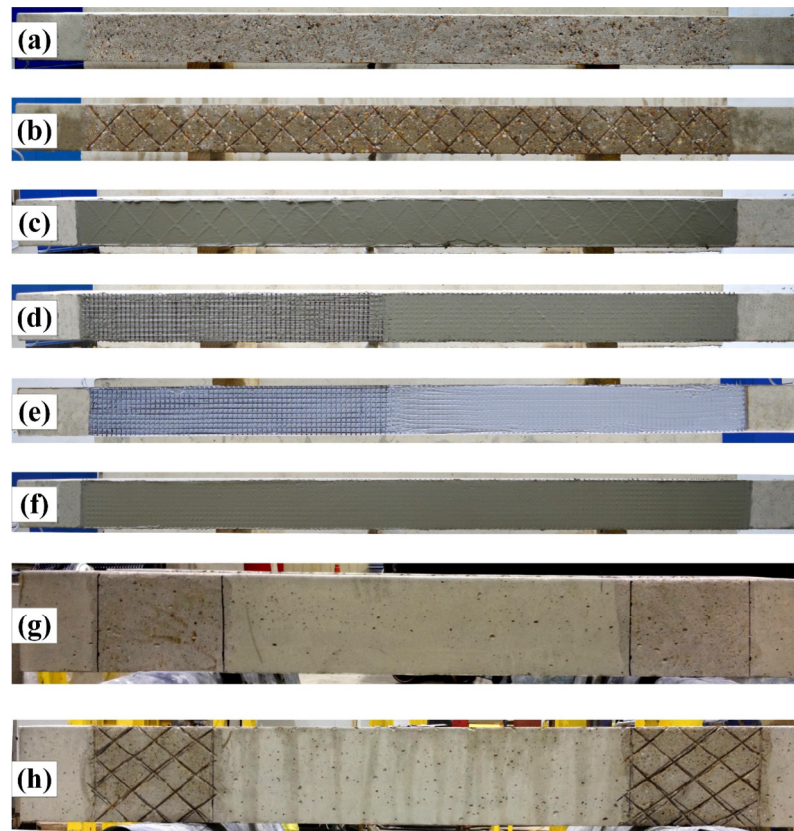
Fig. 5. Strengthening procedure; (a) surface preparation of FRP-strengthened beams, (b) surface preparation of TRM-retrofitted beams, (c) application of first layer of mortar, (d) application of first layer of TRM, (e) application of the first layer of FRP, (f) application of final layer of mortar for TRM reinforced specimens, (g) surface preparation of FRP U-shaped jacket, (h) surface preparation for TRM U-shaped jacket.
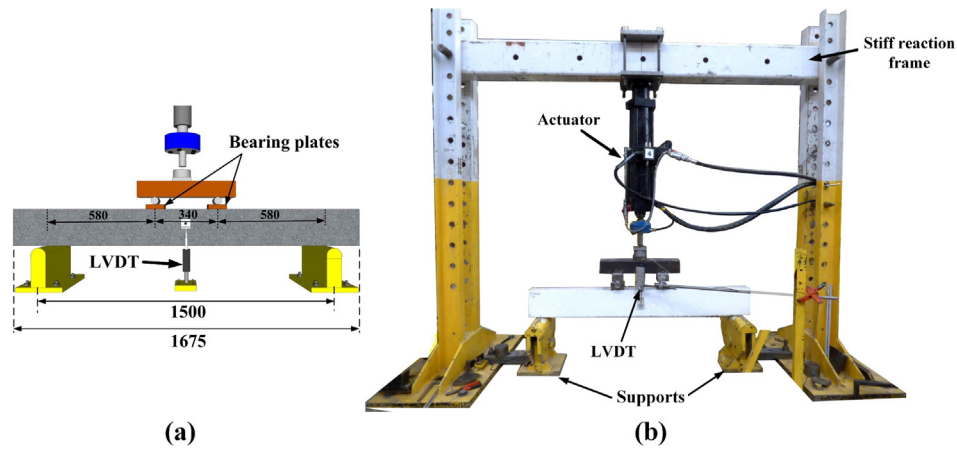
Fig. 6. (a) front view (dimensions in mm), (b) test setup (four-point bending).

Table 3
Summary of test results.

Specimens name	Load (kN)			Deflection (mm)			(7) Capacity increase (%)	(8) Failure mode[a]
	(1) Crack (P_{cr})	(2) Yield (P_y)	(3) Ultimate (P_u)	(4) Crack (δ_{cr})	(5) Yield (δ_y)	(6) Ultimate (δ_u)		
CON	9.8	30.1	34.6	1.06	6.1	30	–	CC
TRM-retrofitted								
M1_C	10	35.6	39.0	0.98	7.3	13.2	12.7	S
M1_CCo	11.6	37	41.3	0.95	6.8	13.6	19.4	ID
M3_C	12.8	43	55.3	1	7.6	14.7	59.8	D
M5_C	16	57.2	62.2	0.76	6.7	8.6	79.8	D
M7_BCo	10.5	38.5	46.9	0.77	7.1	18.4	35.5	FR
M7_G	9.8	40.2	43.2	0.77	7.7	10.3	24.9	FR
M3_C_EA	12	41.3	57.1	1	7	18.4	65.0	DS
FRP-retrofitted								
R1_C	11.8	38.1	43.9	1	6.8	16	26.9	D
R3_C	11.3	51.1	60.4	0.64	8.1	13.7	74.6	D
R7_BCo	13.4	43.7	54.2	1	7.1	24.9	56.6	FR
R7_G	10	41.5	48.2	1	7.9	18.4	39.3	FR
R3_C_EA	11.6	50.7	83.7	1	7.6	26	141.9	FR

[a] CC: Concrete crushing; S: slippage and partial rupture of the fibres through the mortar; ID: TRM debonding at the textile/mortar interface (inter-laminar shearing); D: TRM debonding from concrete substrate; FR: fibres rupture; DS: Debonding of TRM from concrete substrate, followed by slippage of the fibres at the region where the longitudinal TRM meets the TRM U-jacket.

The effect of strengthening was more pronounced during Stages II and III, where development of flexural cracks was in progress. In specific, during Stage II both steel and TRM reinforcement were activated in tension and contributed to the increase of the beam's flexural resistance. In Stage III, the contribution of the steel reinforcement remained almost constant (increased marginally due to steel hardening) due to steel yielding and the further activation of TRM/FRP in tension became the main mechanism contributing to the flexural resistance increase.

The post-peak behaviour of all retrofitted beams was almost identical; after failure, the load dropped to the levels of the unretrofitted (CON) beam's flexural capacity, indicating that the effect of strengthening had totally been lost. After that point, the plastic behaviour of the beams resulted in the development of large deflections under constant residual load. The tests were terminated when a mid-span deflection of 40 mm was reached (specimen CON was tested up to 80 mm, when the longitudinal steel reinforcement was fractured).

3.2. Ultimate loads and failure modes

The values of maximum loads and the observed failure modes of all tested beams are presented in Table 3, supported by Fig. 8.

The reference beam (CON) failed in flexure after the formation of large flexural cracks at the constant moment region. The failure was due to yielding of the tensile reinforcement followed by concrete crushing at the compression zone (Fig. 8a). This type of failure mode is typical for under-reinforced beams. The yield and ultimate load was 30.1 kN and 34.6 kN, respectively, at corresponding mid-span deflection of 6.1 mm and 30.0 mm, respectively.

All FRP strengthened beams also failed in flexure at loads substantially higher than the control beam (Table 3). The ultimate load recorded for specimens R1_C, R3_C, R7_BCo, R7_G and R3_C_EA was 43.9, 60.4, 54.2, 48.2 and 83.7 kN, respectively. Thus, the contribution of various FRP strengthening systems in increasing the flexural capacity was 26.9%, 74.6%, 56.6%, 39.3% and 141.9%, respectively.

Two distinct failure modes were observed in the FRP-retrofitted beams. Specimens retrofitted with one and three layers of carbon-fibre reinforcement (R1_C and R3_C), failed due to debonding of the FRP composite from the concrete surface. Debonding was initiated from an intermediate shear crack (Fig. 8b, c) which caused debonding of the FRP composite from the concrete and propagated from the mid-span towards the end of the beam. Eventually, the FRP strip completely debonded from the beam's soffit with parts
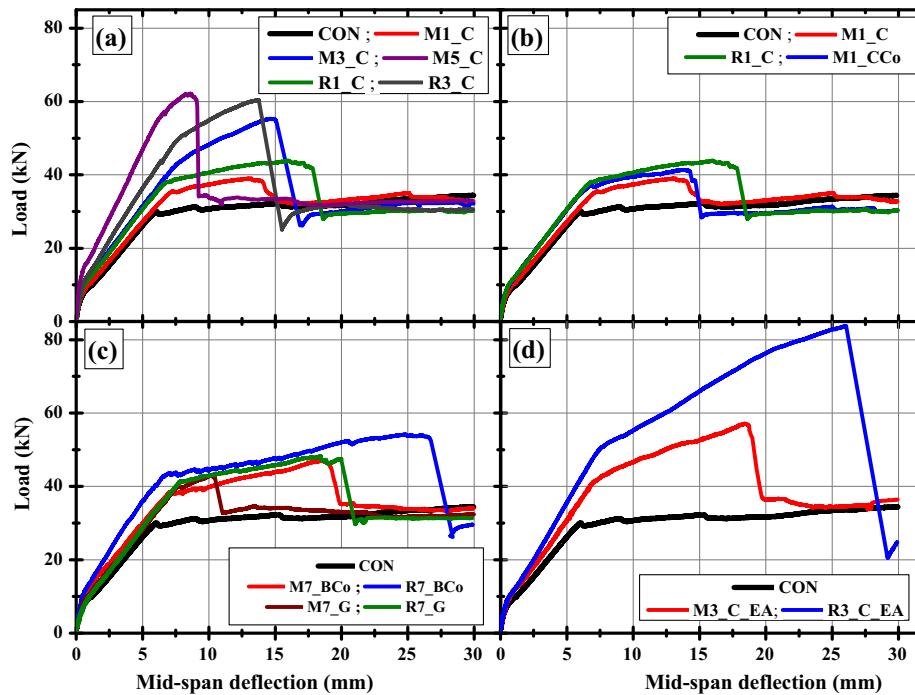
Fig. 7. Load versus mid-span deflection curves of tested beams.

of concrete cover being attached. Details of the failure mode for those beams are also provided in Fig. 8b, c). This kind of failure mode is brittle and quite common for FRP reinforced beams (ACI 2008; FIB 2001) [43,44]. The beams strengthened with seven layers of coated basalt-fibre reinforcement (R7_BCo), seven layers of glass-fibre reinforcement (R7_G), and three layers of carbon-fibre reinforcement anchored at the beam's ends (R3_C_EA), failed due to fibres rupture at the constant moment region of the beam (Fig. 8d–f).

Similar to the FRP-retrofitted beams, all specimens strengthened with TRM failed in flexure after displaying flexural strength considerably higher compared to the control specimen. The maximum load recorded for specimens M1_C, M1_CCo, M3_C, M5_C, M7_BCo, M7_G and M3_C_EA was 39.0, 41.3, 55.3, 62.2, 46.9, 43.2 and 57.1 kN, respectively, which yields 12.7%, 19.4%, 59.8%, 79.8%, 35.5%, 24.9% and 65.0% increase in the flexural capacity, respectively.

Five different failure modes were observed in the TRM-retrofitted beams depending on the number of TRM layers and the textile fibres material:

– Loss of composite action due to slippage of the fibres within the mortar accompanied by partial rupture of the fibres, at a single crack within the maximum moment region (Fig. 8g). This type of failure mode was not brittle (see the post-peak curve in Fig. 7) and was observed in specimen M1_C which received one layer of dry carbon-fibre textile. A progressive load-drop was recorded as a result of the fibres slippage through the cement matrix (Fig. 7a). This type of failure mode was consistent with that observed in [12] in TRM to concrete bond tests, for the same number of TRM layers and the same textile fibre materials (i.e. dry carbon).
– Debonding of TRM due to fracture the surface at the textile-mortar interface. This kind of failure mode was observed in specimen M1_CCo (strengthened with one layer of coated carbon fibre-textile). Debonding was initiated at the intermediate

shear crack and propagated towards the end of the beam (Fig. 8h). This kind of failure, which can also be described as interlaminar shearing [44], is attributed to the effect of coating. Coating the textile with epoxy leads to a strong bond between the inner and the outer filaments of each roving, which increases the rigidity of the textile in both directions and creates strong joints in the junctions between the longitudinal and transversal fibre rovings. As a result, failure due to slippage of the fibre through the mortar was prevented, and damage was shifted to the textile-mortar interface, which was the weakest among all interfaces. The same failure mode was also observed in [12] in TRM to concrete bond tests for the same number of TRM layers and the same textile fibre materials. A detailed picture of the TRM failure surface is also presented in Fig. 8h.

– Debonding of TRM from the concrete surface accompanied with part of the concrete cover. The debonding initiated from an intermediate shear crack (Fig. 8i) and propagated from the constant moment zone towards one end of the TRM reinforcement. Eventually TRM debonded form the concrete surface with a part of concrete cover being peeled off (Fig. 8i). This failure mode was observed in specimen M3_C and M5_C, and it was the same as in its counterpart FRP-retrofitted beam (R3_C). Again, the same failure mode was also observed in [12], in TRM to concrete bond tests for three layers of the same materials.
– Fibres rupture in the region of maximum moment (Fig. 8j, k). This type of failure mode was noted in specimens M7_BCo and M7_G, strengthened with seven layers of coated basalt and glass-fibre textile, respectively.
– Debonding of TRM from the concrete substrate (part of the concrete cover was also included) at an intermediate shear crack (Fig. 8l), followed by slippage of the fibres at a different region. This failure mode was observed in specimen M3_C_EA, retrofitted with three layers of dry carbon-fibre textile and received TRM U-jackets at their ends to provide anchorage. It is noted that providing U-jacket at the ends of the beam prevented debonding of TRM, but slippage of fibres finally occurred at
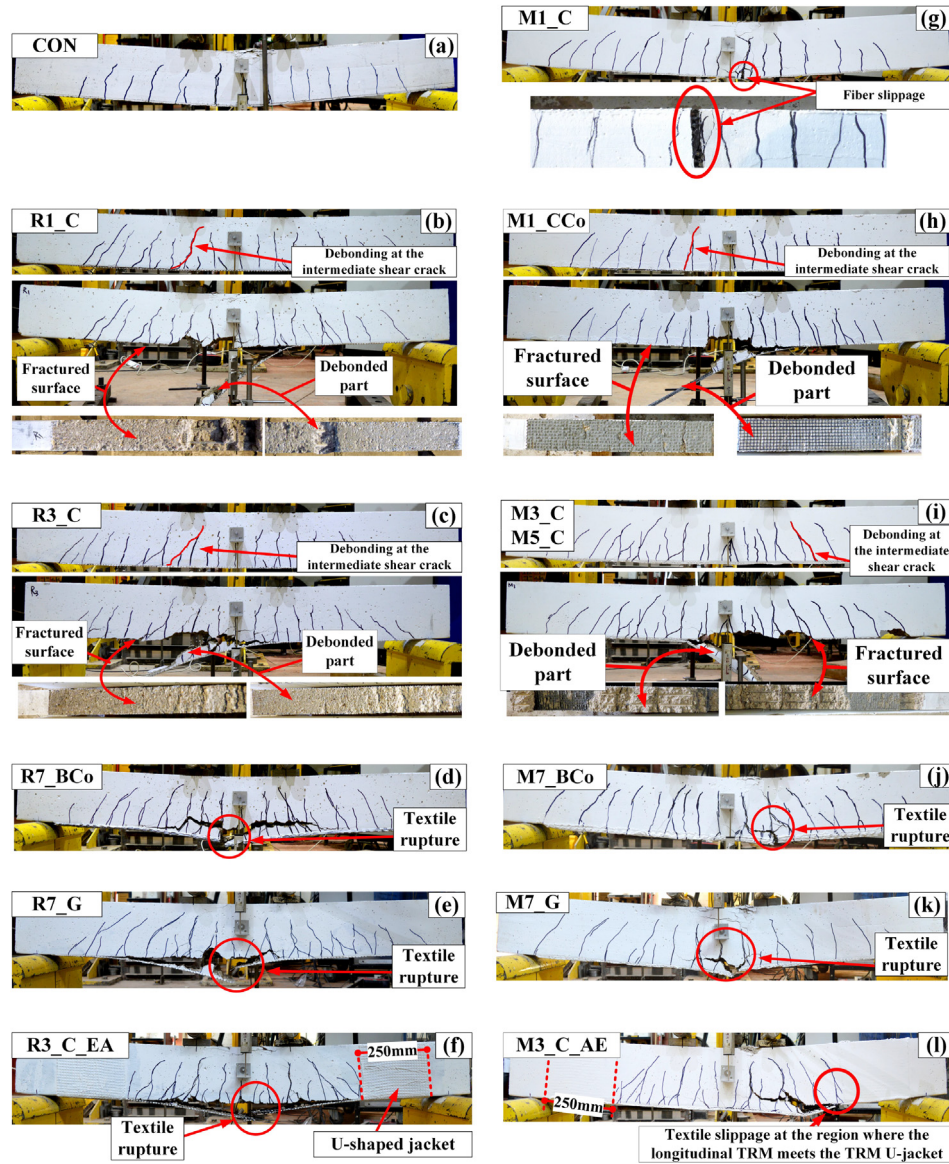
Fig. 8. Failure mechanisms and details of failure modes of tested beams.

the region where the longitudinal TRM meets the TRM U-jacket (Fig. 8l). The same failure mode was also observed in [12], in TRM to concrete bond tests for the same number of TRM layers and the same textile fibre materials.

3.3. Bending stiffness

The bending stiffness of the tested beams at several stages (pre-cracking, cracking and post-yielding) is reported in Table 4. It was calculated form the load versus mid-span deflection curves as the tangent stiffness of the pre-cracking, cracking and post-yielding stages. As shown in Table 4, the application of strengthening (TRM or FRP) enhanced the cracking and post-yielding stiffness compared to the reference beam. It is noted that the increase in the cracking and post-yielding stiffness was sensitive to the investigated parameters such as the strengthening system (TRM or FRP), the number of TRM/FRP layers, the textile fibre material, and the strengthening configuration.

Table 4
Comparison of stiffness at pre-cracking, cracking and post-yielding stage.

Specimens	Pre-cracking stiffness (kN/mm)	Cracking stiffness (kN/mm)	Post-yielding stiffness (kN/mm)
CON	9.2	4.0	0.19
TRM-retrofitted			
M1_C	10.2	4.1 (1)[*]	0.58 (206)[*]
M1_CCo	12.2	4.3 (8)[*]	0.63 (236)[*]
M3_C	12.8	4.6 (14)[*]	1.73 (820)[*]
M5_C	21.1	6.9 (72)[*]	2.63 (1298)[*]
M7_BCo	17.7	4.4 (10)[*]	0.74 (295)[*]
M7_G	12.9	4.4 (9)[*]	1.15 (513)[*]
M3_C_EA	12.0	4.9 (21)[*]	1.39 (636)[*]
FRP-retrofitted			
R1_C	11.8	4.5 (13)[*]	0.63 (235)[*]
R3_C	17.7	5.3 (32)[*]	1.66 (782)[*]
R7_BCo	13.4	5.0 (23)[*]	0.59 (213)[*]
R7_G	10.0	4.6 (13)[*]	0.64 (239)[*]
R3_C_EA	11.6	5.9 (47)[*]	1.79 (853)[*]

[*] Percentage increase (%) in stiffness with respect to CON included in parentheses.

4. Discussion

All strengthened specimens responded as designed and failed by the loss of strengthening after yielding of the internal steel reinforcement. On the basis of the various parameters investigated in this experimental programme, an examination of the results (Table 3) in terms of strength, stiffness and failure modes, revealed the following information.

4.1. Number of strengthening layers

The effect of the number of layers on the beams flexural capacity was investigated for the case of dry carbon-fibre textiles, and is depicted in Fig. 7a supported by Fig. 9a. For FRP-strengthened beams, tripling the amount of reinforcement (from one to three layers) resulted in almost proportional increase in the flexural capacity, namely 2.8 times. The corresponding enhancement in the TRM-strengthened beams was equal to 4.7 times (non-proportional increase). To further investigate the effect of increasing the number of TRM layers on the flexural capacity increase, a beam strengthened with five TRM layers was also tested. As shown in Fig. 9a, applying five layers of TRM resulted in 6.3 times increase compared to one TRM layer. The non-proportional increase observed in the TRM strengthened (especially for the transition from one to more layers) is associated to the different failure modes observed, as described below.

The cracking and post-yielding stiffness were enhanced by increasing the number of layers for both strengthening systems in an identical manner (Fig. 9b). In the FRP-strengthened beams, tripling the number of layers resulted in an increase of 1.2 and 2.7 times in the cracking and post-yielding stiffness, respectively. The corresponding enhancement in TRM-retrofitted beams was similar, namely 1.1 and 3 times, respectively. It seems that the increase in the post-yielding stiffness was almost directly proportional to the number of layers even for the case of M5_C (4.5 times compared with M1_C). This is attributed to the fact that the only mechanism contributing to the flexural capacity increase is the activation of the externally applied materials in tension.

The failure mode of FRP strengthened specimens was not sensitive to the number of layers; it was always debonding of FRP from the concrete substrate including part of concrete cover (Fig. 8a and b). However, in the case of TRM-retrofitted beams, the failure mode was sensitive to the number of layers. In particular, the failure mode altered when three or five layers of dry carbon-fibre textile were applied instead of one. With 3 or 5 layers, slippage of the fibres through the mortar was prevented and the failure, as in the case of FRP, was attributed to TRM debonding including part of concrete cover (Fig. 8i). This behaviour is identical with the observations made by Tetta et al. 2016 Tetta et al. 2016

[16] in shear strengthening of RC beams with TRM when the number of layers increased from 1 to 2, but also by Raoof et al. [12] in double-lap shear TRM-to-concrete bond tests. Improved mechanical interlock between the increased number of textile layers and the surrounding mortar is believed by the authors to be the main reason for this behaviour.

4.2. Textile-fibres coating

Beam M1_C, strengthened with one TRM layer of dry (uncoated) carbon-fibre textile, failed prematurely due to local slippage of the fibres through the mortar. For this reason, it was decided to retrofit a beam using the same textile but with coated fibres (M1_CCo). As a result, the flexural capacity was further increased by 52% (compared to beam M1_C). Additionally, the failure mode was changed from slippage of the fibres through the mortar to debonding of TRM due to fracture at the textile-mortar interface (Fig. 8h; interlaminar shear failure [44]). Such a failure mode was also observed in bond tests conducted by the authors when the same textile with the same coating was used [12]. As illustrated in Fig. 7b and Fig. 10a-c, although the performance of the beam M1_C was poor compared to its counterpart FRP-strengthened specimen (R1_C), when coated textile was used, the behaviour of TRM became comparable to FRP. Coating the textile leads to improved bond between the inner and the outer filaments of each roving of the textile. Hence, the textile develops higher tensile stresses, and the matrix is called to transfer higher shear stresses, which leads to shear failure of the mortar (interlaminar shearing).

4.3. Textile-fibres material

According to the results (Fig. 7c and Fig. 10a), in both TRM and FRP strengthening systems, the highest flexural capacity increase was achieved in the beams retrofitted by the coated basalt-fibre reinforcement. In TRM-strengthened beams, specimen M7_BCo recorded a 45% higher capacity increase compared to specimen M1_CCo with equivalent axial stiffness of the strengthening layers, and beam M7_G recorded a 49% higher capacity increase compared to beam M1_C. Note that the above comparisons were made on the basis of similar textile surface conditions (dry or coated textiles). Similarly, in FRP-retrofitted beams, the flexural capacity increase of beam R7_BCo was 52% and 30% higher than that of beams R1_C and R7_G, respectively. This disparity in the flexural capacity increase between beams with external reinforcement of approximately the same axial stiffness, can be attributed to the influence of the numbers of layers (one layer of TRM reinforcement was less effective than multiple No. of layers as discussed in Section 4.1) and to the fact that the basalt-fibre textile was coated, which was beneficial at least in the case of the TRM strengthening system.
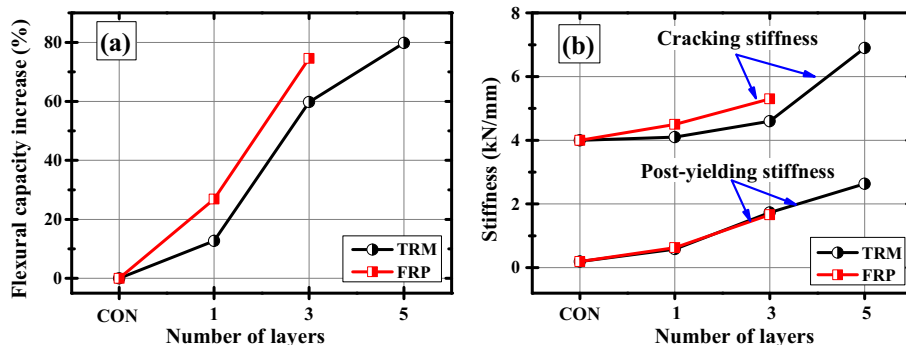
Fig. 9. Effect of number of layers on: (a) the ultimate flexural capacity; and (b) the cracking stiffness, and post-yielding stiffness.
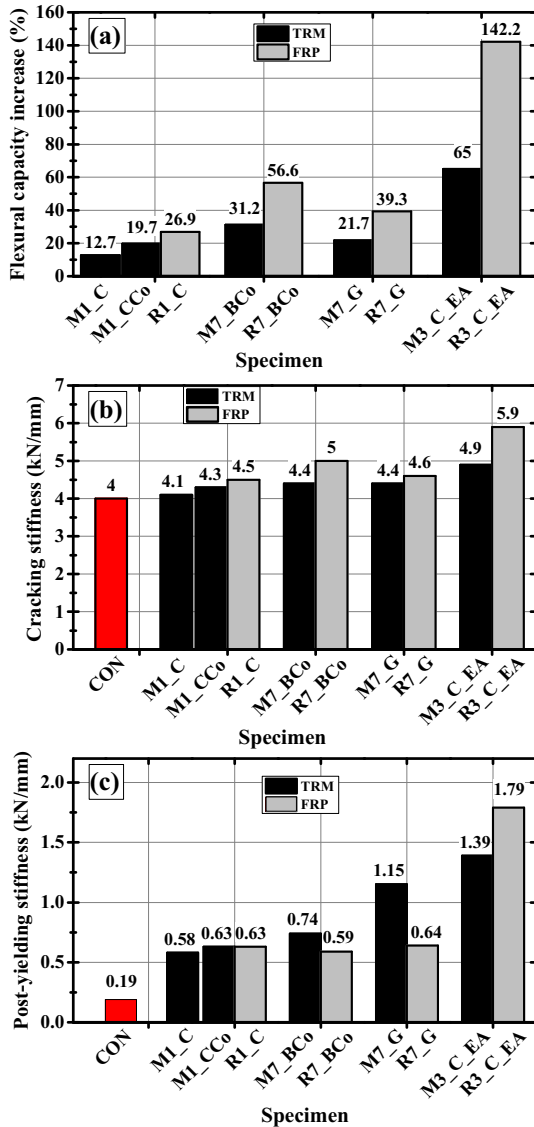
Fig. 10. Comparison of TRM vs FRP strengthened beams: (a) flexural capacity; (b) cracking.

4.4. End-anchorage with U-jackets

An end-anchorage system comprising U-jackets at both ends of the beams was applied only for specimens strengthened with three layers of carbon TRM or FRP, as a means of preventing premature debonding from the concrete substrate. As illustrated in Fig. 10a, in the case of beam R3_C_EA, the strengthening efficiency was substantially increased (by 90%) compared to the beam without end-anchorage (R3_C). However, this enhancement was limited in the case of the TRM strengthened beam (only 9%). The difference in the behaviour between specimens R3_C_EA and M3_C_EA is attributed to the difference in the failure mode observed. Beam R3_C_EA failed due to rupture of the textile fibres (Fig. 8f) achieving full composite action. In contrary, in beam M3_C_EA even if TRM debonding was prevented, a full composite action was not achieved due to slippage of the textile fibres at the junction where the longitudinal TRM meets the U-jacket (Fig. 8l).

4.5. TRM vs FRP effectiveness factor

Table 5 reports the values of the TRM versus FRP effectiveness factor (k), which is defined as the ratio of the flexural capacity increase achieved by TRM to the increase achieved by the equivalent FRP. This factor varied between 0.46 and 0.80 for the different parameters examined in this study.

Increasing the number of dry carbon-fibre textile layers from one to three, resulted in enhancement of the effectiveness factor from 0.47 to 0.80, which was associated to the change in the failure mode of TRM retrofitted beams (from slippage of the fibres to debonding of from the concrete substrate). Coating the carbon textile with epoxy resin in the case of 1 TRM layer increased the k factor from 0.47 to 0.73, as a result of prevention of fibres slippage.

The effectiveness factor for the specimens retrofitted with either coated basalt, or glass-fibre textiles was the same and equal to 0.63. In this case, although both FRP and TRM-retrofitted specimens failed due to rupture of textile fibres, the reduced effectiveness of TRMs can be attributed to the lower tensile strength of TRM composites compared to FRPs (as shown from the results of the coupons tensile tests).

Finally, in terms of strengthening configuration, specimen M3_C_EA recorded an effectiveness factor of 0.46. This low value of k factor was due to the development of slippage at the junction where the longitudinal TRM reinforcement meets the U-jacket (Fig. 8l). This slippage considerably reduced the TRM effectiveness and prevented a full composite action.

5. Analytical calculations

To calculate the effective stress, σ_{eff}, of the TRM or FRP reinforcement, an inverse analysis method was used. The effective stress is defined here as the tensile stress of the composite material in the region of maximum moments at the instant of ultimate load. By using the experimental values of the flexural moment of resistance, $M_{u,\exp}$ (Table 5), a standard cross section analysis, described in fib *Model Code 2010* [44], was performed for each of the retrofitted beams. The procedure for the calculation of σ_{eff} in this method was built on the equilibrium of internal forces and strains compatibility. Also, the following assumptions were adopted:

- There is perfect bond between the FRP/TRM strengthening layers and the concrete substrate.
- The ultimate compressive strain of concrete (ε_{cu}) is 0.0035.
- The strengthening material behaves linearly up to failure.

It is worth mentioning that the mechanical properties of the external reinforcement (E_f and f_{fu}) were taken from the coupon tests described in Section 2.2 (Table 2). The experimental values of the effective stress, $\sigma_{eff,\exp}$, resulted from the inverse analysis, are presented in Table 5. As shown on the same Table, the ratio of the effective stress ($\sigma_{eff,\exp}$) to the ultimate stress obtained from coupon test (f_{fu}) was always less than one, except for the beam R3_C_EA (probably due to the effect of the end-anchorage system).

The theoretical values of the debonding stress of the composite material, $f_{fbm,theor}$, were calculated according to Eq. (1) (fib Model Code 2010 [45] equation for flexural strengthening with FRP) and are presented in Table 5 (without safety factors). Note that Eq. (1) can only be used for debonding failures occurring at the concrete substrate.

$$f_{fbm} = k_c k_m k_b \beta_\ell \sqrt{\frac{2E_f}{t_f} f_{cm}^{2/3}} \tag{1}$$

In the above equation, f_{fbm} is the mean debonding stress of the composite material; k_c is the intermediate crack factor and equal to 2; k_m is the matrix factor and equal to 0.25 for the case of epoxy bonded CFRP system (the same value was used here for the case of the carbon-TRM system); k_b is the shape factor; β_ℓ is the length

Table 5
Effectiveness factor, experimental values of ultimate moment capacity and effective stress in TRM/FRP reinforcement.

Specimen	TRM vs FRP effectiveness factor, k	$M_{u,exp.}$* kN.m	$\sigma_{eff,exp.}$**	F.M.***	f_{fu}^+ (MPa)	$\sigma_{eff,exp.}/f_{fu}$	$f_{fbm,theor}^{++}$	$\sigma_{eff,exp.}/f_{fbm,theor}$	$f_{f,bond}^a$	F.M.[b]	$f_{f,bond}/f_{fu}$
CON	–	10.03	–	–			–	–			
TRM-retrofitted											
M1_C	0.47	11.31	1368	S	1518	0.90	n.a.	n.a.	915	S	0.75
M1_CCo	0.72	12.01	1825	ID	2843	0.64	n.a.	n.a.	1572	ID	0.55
M3_C	0.80	16.04	1434	D	1518	0.94	1466	0.98	790	D	0.55
M5_C	n.a.	18.04	1126	D	1518	0.74	1136	0.99	n.a.	D	n.a.
M7_BCo	0.63	13.60	1019	FR	1190	0.86	n.a.	n.a.	1046[c]	FR[c]	0.88
M7_G	0.63	12.53	658	FR	794	0.83	n.a.	n.a.	709[c]	FR[c]	0.89
M3_C_EA	0.46	16.56	1501	D	1518	0.99	n.a.	n.a.	877	D	0.58
FRP-retrofitted											
R1_C	n.a.	12.73	2190	D	2936	0.75	2995	0.73	n.a.	n.a.	n.a.
R3_C	n.a.	17.52	1796	D	2936	0.61	1729	1.04	n.a.	n.a.	n.a.
R7_BCo	n.a.	15.72	1493	FR	1501	0.99	n.a.	n.a.	n.a.	n.a.	n.a.
R7_G	n.a.	13.98	914	FR	1019	0.90	n.a.	n.a.	n.a.	n.a.	n.a.
R3_C_EA	n.a.	24.30	3110	FR	2936	1.06	n.a.	n.a.	n.a.	n.a.	n.a.

* Ultimate moment capacity obtained experimentally.
** Effective stress in TRM/FRP reinforcement calculated based on experimental results.
*** Failure mode of strengthened beams (see Table 3).
+ Ultimate stress in the textiles fibres obtained from coupon test (Table 2).
++ Mean debonding stress in TRM/FRP reinforcement calculated according to Eq. (1).
[a] Average stress in TRM reinforcement obtained from bond test included in Raoof et al. (2016) [12].
[b] Failure mode observed in bond test included in Raoof et al. (2016) [12].
[c] Bond tests currently carried on.

factor which can be taken equal to 1; E_f is the elastic modulus the composite material (obtained from coupon test); t_f is the equivalent thickness of the textile and f_{cm} is the concrete compressive strength; and the shape factor (k_b) was calculated from Eq. (2) below:

$$k_b = \sqrt{\frac{2 - b_f/b}{1 + b_f/b}} \geqslant 1 \qquad (2)$$

where; b_f is the width of the composite, and b is the width of the beam.

Eq. (1) was used here to calculate both FRP and TRM debonding stresses in the cases of debonding failures. A comparison of the stresses calculated according to Eq. (1) with the experimental data is presented in Table 5. It was found that the debonding stress calculated by Eq. (1) is in a good agreement with the experimental results of that beams reinforced with high FRP and TRM reinforcement ratio (M3_C, M5_C and R3_C) and failed due to debonding of FRP or TRM from the concrete substrate including part of the concrete cover.

Fig. 11 shows the relationship between the effective stress obtained experimentally $\sigma_{eff,exp.}$ and the product $\rho_f E_f$; together with the curve corresponding to Eq. (1). Where ρ_f is the textile fibres reinforcement ratio ($\rho_f = A_f/bh$), and E_f is the modulus of elasticity of the composite material obtained from coupon tests. It is clear from this figure that the effective stress developed in the textile fibres reinforcement is inversely proportional to the product $\rho_f E_f$ when the failure is associated to debonding of the externally bonded reinforcement, regardless the binding material (epoxy resin or mortar). This trend of the effective stress is consistent with the trend of the theoretical stress calculated by Eq. (1) and shown in Fig. 11a, and b (dash line).

Based on the above findings, in design of flexural retrofitting with TRM system, the effective stress can be the minimum value obtained from coupon tests (f_{fu}) and Eq. (1), applying the same safety factors as in FRP systems until more data become available and a semi-probabilistic approach can be applied to obtain TRM-specific safety factors. Nevertheless, this design approach is suggested to be used only when the failure mode is either TRM debonding at an intermediate crack or fibres rupture. According to the results of the present experimental study, this applies when more than 2 TRM layers are used for retrofitting. It is evident that more experimental data is required for a refined design model which will consider all different failure modes observed, including the slippage of the TRM reinforcement in flexural cracks.
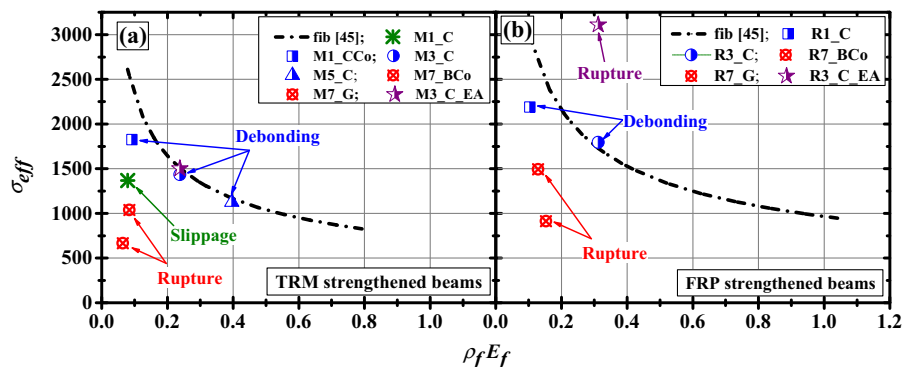
Fig. 11. Experimentally obtained effective stress versus $\rho_f E_f$ and comparison with the theoretical formula suggested by *fib* [45]; (a) TRM-strengthened beams; (b) FRP-strengthened beams.

Table 5 also compares the effective stress in the TRM composite ($\sigma_{eff,exp}$) with the debonding stress obtained through direct shear-bond tests ($f_{f,\ bond}$) in the study of Raoof et al. 2016 [12]. The comparison is made on the basis of the same number of TRM layers used in both studies, with the same materials. The $f_{f,\ bond}$ values used for the comparison correspond to 200 mm bond length, which was found to be the effective bond length (in which the bond strength is not significantly increased beyond this length). Although identical failure modes were noted in both flexural and bond tests (for identical specimens having the same textile fibre materials and number of TRM layers) the debonding stresses recorded at failure were lower in the bond tests, leading to lower utilisation of the textile fibres reinforcement.

6. Conclusions

This study investigated experimentally the performance of TRM and FRP composite in flexural strengthening of RC beams. Several parameters were examined namely: (a) the strengthening material (TRM and FRP); (b) the number of FRP/TRM layers; (c) the textile surface condition; (d) the textile-fibre materials and (e) the end anchorage system. The obtained results revealed the following conclusions:

1. The effectiveness of TRM system in increasing the loading carrying capacity of retrofitted beams was less than that of FRP. Nevertheless, TRM effectiveness was sensitive to the number of layers. It was found that the effectiveness factor increased from 0.47 to 0.80 when the number of TRM layers increased from 1 to 3.
2. Coating the carbon fibres textile with epoxy adhesive significantly enhanced the performance of TRM materials. When one layer of coated carbon textile was used instead of one layer of dry carbon textile, the flexural capacity gain increased from 12.7 to 19.7% (about 55% enhancement).
3. Different textile fibres materials (carbon, coated basalt, and glass) having approximately the same axial stiffness resulted in different flexural capacity increases. In both strengthening systems, seven coated basalt- fibre textile layers recorded the highest flexural capacity increase, followed by seven dry glass- fibre textile layers, and finally by one carbon- fibre textile layer. This variance in the performance was related to the effect of number of layers (in both FRP and TRM strengthening systems), but also to the textile surface condition (dry or coated textiles) in TRM strengthening system.
4. Providing end-anchorage with U-jackets to FRP-retrofitted beams resulted in 90% enhancement in the flexural capacity compared to non- anchorage beam. However, the corresponding enhancement in TRM-retrofitted beam was limited (9%) and was attributed to the presence of slippage of the textile at the U-jacket – longitudinal TRM sheets.
5. Two types of failure mode were observed in the FRP-retrofitted beams, these failure modes were: debonding from concrete substrate (for specimens M1_C and M3_C), and fibres rupture at the constant moment zone (for specimens M7_BCo, M7_G and M3_C_EA). Whereas, in the TRM-retrofitted beams five different failure modes were observed, namely: slippage of the rovings through the surrounding cement mortar (specimen M1_C), fracture the surface at the textile- matrix interface (interlaminar debonding- specimen M1_CCo), debonding of TRM from the concrete with peeling off parts concrete cover (specimen M3_C and M5_C), and rupture of the textile fibres at the constant moment zone (M7_BCo and M7_G). These failure modes were found to be sensitive to the number of TRM layers, the textile fibres materials (carbon, coated basalt or glass fibres), and the textile surface condition (dry or coated fibres).
6. For both strengthening systems (TRM and FRP), the cracking and post-yielding stiffness of strengthened beams was substantially enhanced compared to the unstrengthened beam (up to 72% and 1298%, respectively).
7. A formula proposed by *fib 2010* [45] was used to predict the debonding stress in FRP reinforced for those specimens failed due to debonding of FRP from concrete substrate. This formula was also used to predict the debonding stress of TRM reinforcement for those specimens that have same failure mode (i.e. debonding). It was found that this formula is in a good agreement with the effective stress calculated based on the experimental results providing that TRM properties are obtained from coupon tests. The above-mentioned conclusions should be treated carefully. They are based on a limited number of tests on half-scale beams and specific type of textile fibre materials. More research is required including different types of textile materials and full-scale beams. This would also help to confirm the reliability of existing design models for FRP or the development of new reliable ones.

References

[1] D.A. Bournas, P.V. Lontou, C.G. Papanicolaou, T.C. Triantafillou, Textile-reinforced mortar versus fiber-reinforced polymer confinement in reinforced concrete columns, ACI Struct. J. 104 (6) (2007).

[2] T.C. Triantafillou, C.G. Papanicolaou, Shear strengthening of reinforced concrete members with textile reinforced mortar (TRM) jackets, Mater. Struct. 39 (1) (2006) 93–103.

[3] W. Brameshuber, Report 36: Textile Reinforced Concrete-State-of-the-Art Report of RILEM TC 201-TRC, RILEM Publications, 2006.

[4] C. Carloni, D.A. Bournas, F.G. Carozzi, T. D'Antino, G. Fava, F. Focacci, Fiber Reinforced Composites with Cementitious (inorganic) Matrix. Design Procedures for the Use of Composites in Strengthening of Reinforced Concrete Structures, Springer, 2016. p. 349–392.

[5] S.M. Raoof, D.A. Bournas, Bond between TRM versus FRP composites and concrete at high temperatures, Compos. Eng. (2017), http://dx.doi.org/10.1016/j.compositesb.2017.05.064.

[6] Z.C. Tetta, D.A. Bournas, TRM vs FRP jacketing in shear strengthening of concrete members subjected to high temperatures, Compos. B Eng. 106 (2016) 190–205.

[7] O. Awani, A. El Refai, T. El-Maaddawy, Bond characteristics of carbon fabric-reinforced cementitious matrix in double shear tests, Constr. Build. Mater. 101 (2015) 39–49.

[8] T. D'Antino, C. Carloni, L. Sneed, C. Pellegrino, Matrix–fiber bond behavior in PBO FRCM composites: A fracture mechanics approach, Eng. Fract. Mech. 117 (2014) 94–111.

[9] A. D'Ambrisi, L. Feo, F. Focacci, Experimental analysis on bond between PBO-FRCM strengthening materials and concrete, Compos. B Eng. 44 (1) (2013) 524–532.

[10] D'Antino T, Pellegrino C, Carloni C, Sneed LH, Giacomin G, editors. Experimental analysis of the bond behavior of glass, carbon, and steel FRCM composites. Key Engineering Materials; 2014: Trans Tech Publ.

[11] L. Ombres, Analysis of the bond between Fabric Reinforced Cementitious Mortar (FRCM) strengthening systems and concrete, Compos. B Eng. 69 (2015) 418–426.

[12] S.M. Raoof, L.N. Koutas, D.A. Bournas, Bond between textile-reinforced mortar (TRM) and concrete substrates: Experimental investigation, Compos. B Eng. 98 (2016) 350–361.

[13] L.H. Sneed, T. D'Antino, C. Carloni, Investigation of bond behavior of PBO fiber-reinforced cementitious matrix composite-concrete interface, ACI Mater. J. 111 (1–6) (2014).

[14] C.T.M. Tran, B. Stitmannaithum, T. Ueda, Investigation of the bond behaviour between PBO-FRCM strengthening material and concrete, Journal of Advanced Concrete Technology. 12 (12) (2014) 545–557.

[15] G. Loreto, S. Babaeidarabad, L. Leardini, A. Nanni, RC beams shear-strengthened with fabric-reinforced-cementitious-matrix (FRCM) composite, International Journal of Advanced Structural Engineering (IJASE). 7 (4) (2015) 341–352.

[16] Z.C. Tetta, L.N. Koutas, D.A. Bournas, Textile-reinforced mortar (TRM) versus fiber-reinforced polymers (FRP) in shear strengthening of concrete beams, Compos. B Eng. 77 (2015) 338–348.

[17] E. Tzoura, T. Triantafillou, Shear strengthening of reinforced concrete T-beams under cyclic loading with TRM or FRP jackets, Mater. Struct. 49 (1–2) (2016) 17–28.

[18] Z.C. Tetta, L.N. Koutas, D.A. Bournas, Shear strengthening of full-scale RC T-beams using textile-reinforced mortar and textile-based anchors, Compos. B Eng. 95 (2016) 225–239.

[19] O. Awani, T. El-Maaddawy, A. El Refai, Numerical simulation and experimental testing of concrete beams strengthened in shear with fabric-reinforced cementitious matrix, Journal of Composites for Construction. 20 (6) (2016) 04016056.

[20] D.A. Bournas, T.C. Triantafillou, K. Zygouris, F. Stavropoulos, Textile-reinforced mortar versus FRP jacketing in seismic retrofitting of RC columns with continuous or lap-spliced deformed bars, Journal of Composites for Construction. 13 (5) (2009) 360–371.

[21] D. Bournas, T. Triantafillou, Bar buckling in RC columns confined with composite materials, Journal of Composites for Construction. 15 (3) (2010) 393–403.

[22] D. Bournas, T. Triantafillou, Bond strength of lap-spliced bars in concrete confined with composite jackets, Journal of Composites for Construction. 15 (2) (2011) 156–167.

[23] D.A. Bournas, T.C. Triantafillou, Biaxial bending of reinforced concrete columns strengthened with externally applied reinforcement in combination with confinement, ACI Structural Journal. 110 (2) (2013) 193.

[24] L. Ombres, S. Verre, Structural behaviour of fabric reinforced cementitious matrix (FRCM) strengthened concrete columns under eccentric loading, Compos. B Eng. 75 (2015) 235–249.

[25] L. Koutas, S. Bousias, T. Triantafillou, Seismic strengthening of masonry-infilled RC frames with TRM: experimental study, Journal of Composites for Construction. 19 (2) (2014) 04014048.

[26] F. Jesse, S. Weiland, M. Curbach, Flexural strengthening of RC structures with textile-reinforced concrete, Special Publication. 250 (2008) 49–58.

[27] G. Loreto, L. Leardini, D. Arboleda, A. Nanni, Performance of RC slab-type elements strengthened with fabric-reinforced cementitious-matrix composites, Journal of Composites for Construction. 18 (3) (2013) A4013003.

[28] F. Schladitz, M. Frenzel, D. Ehlig, M. Curbach, Bending load capacity of reinforced concrete slabs strengthened with textile reinforced concrete, Eng. Struct. 40 (2012) 317–326.

[29] L.N. Koutas, D.A. Bournas, Flexural strengthening of two-way RC slabs with textile-reinforced mortar: experimental investigation and design equations, Journal of Composites for Construction. 04016065 (2016).

[30] D. Bournas, Strengthening of existing structures: selected case studies, in: T.C. Triantafillou (Ed.), Textile Fibre Composites in Civil Engineering, Elsevier, Woodhead Publishing Limited, 2016, pp. 389–411. Ch. 17.

[31] T.C. Triantafillou, C.G. Papanicolaou, editors. Textile reinforced mortars (TRM) versus fiber reinforced polymers (FRP) as strengthening materials of concrete structures. Proceedings of the 7th ACI International Symposium on Fibre-Reinforced (FRP) Polymer Reinforcement for Concrete Structures; 2005: American Concrete Institute.

[32] L. Ombres, Flexural analysis of reinforced concrete beams strengthened with a cement based high strength composite material, Compos. Struct. 94 (1) (2011) 143–155.

[33] A. D'Ambrisi, F. Focacci, Flexural strengthening of RC beams with cement-based composites, Journal of Composites for Construction. 15 (5) (2011) 707–720.

[34] L. Ombres, Debonding analysis of reinforced concrete beams strengthened with fibre reinforced cementitious mortar, Eng. Fract. Mech. 81 (2012) 94–109.

[35] H.M. Elsanadedy, T.H. Almusallam, S.H. Alsayed, Y.A. Al-Salloum, Flexural strengthening of RC beams using textile reinforced mortar–Experimental and numerical study, Compos. Struct. 97 (2013) 40–55.

[36] S. Babaeidarabad, G. Loreto, A. Nanni, Flexural strengthening of RC beams with an externally bonded fabric-reinforced cementitious matrix, Journal of Composites for Construction. 18 (5) (2014) 04014009.

[37] U. Ebead, K.C. Shrestha, M.S. Afzal, A. El Refai, A. Nanni, Effectiveness of fabric-reinforced cementitious matrix in strengthening reinforced concrete beams, Journal of Composites for Construction. 04016084 (2016).

[38] EN-12390-3, Testing Hardened Concrete–Part 3: Compressive Strength of Test Specimens, Czech Standards Institute, Prague, 2009.

[39] EN-12390-6, Testing Hardened Concrete—Tensile Splitting Strength of Test Specimens, Italian Standardization Board, 2002.

[40] 1015-11 E. 1015-11: Methods of Test for Mortar for Masonry–Part 11. Determination of flexural and compressive strength of hardened mortar Brussels: Comité Européen de Normalisation. 1993

[41] ACI A. 440.3 R-04, Guide Test Methods for Fiber-Reinforced Polymers (FRPs) for Reinforcing or Strengthening Concrete Structures, American Concrete Institute, Farmington Hills, USA, 2004.

[42] J. Orlowsky, M. Raupach, Durability model for AR-glass fibres in textile reinforced concrete, Mater. Struct. 41 (7) (2008) 1225–1233.

[43] ACI Commitee A. 440.2 R-08. Guide for the Design and Construction of Externally Bonded FRP Systems for Strengthening Concrete Structures. 2008.

[44] fib Model Code l. International Federation for Structural Concrete (fib), Vol. 1-Bulletin 55, Vol. 2-Bulletin 56. Lausanne; 2010.

[45] fib Model Code a. Model code for concrete structures. Bulletin 14, 2010; Lausanne; Switzerland. 2010.